

Skyrmion Logic System for Large-Scale Reversible Computation

Maverick Chauwin^{1,2,†}, Xuan Hu^{1,‡}, Felipe Garcia-Sanchez^{3,4}, Neilesh Betrabet,¹
Alexandru Paler,⁵ Christoforos Moutafis⁶, and Joseph S. Friedman^{1,*}

¹*Department of Electrical & Computer Engineering, The University of Texas at Dallas, Richardson, Texas 75080, USA*

²*Department of Physics, École Polytechnique, 91128 Palaiseau, France*

³*Istituto Nazionale di Ricerca Metrologica, 10135 Torino, Italy*

⁴*Departamento de Física Aplicada, Universidad de Salamanca, 37008 Salamanca, Spain*

⁵*University of Transilvania, Brasov 500091, Romania*

⁶*Department of Computer Science, The University of Manchester, Manchester M13 9PL, United Kingdom*



(Received 21 May 2019; revised manuscript received 8 October 2019; published 24 December 2019)

Computational reversibility is necessary for quantum computation and inspires the development of computing systems, in which information carriers are conserved as they flow through a circuit. While conservative logic provides an exciting vision for reversible computing with no energy dissipation, the large dimensions of information carriers in previous realizations detract from the system efficiency, and nanoscale conservative logic remains elusive. We therefore propose a nonvolatile reversible computing system in which the information carriers are magnetic skyrmions, topologically-stable magnetic whirls. These nanoscale quasiparticles interact with one another via the spin Hall and skyrmion Hall effects as they propagate through ferromagnetic nanowires structured to form cascaded conservative logic gates. These logic gates can be directly cascaded in large-scale systems that perform complex logic functions, with signal integrity provided by clocked synchronization structures. The feasibility of the proposed system is demonstrated through micromagnetic simulations of Boolean logic gates, a Fredkin gate, and a cascaded full adder. As skyrmions can be transported in a pipelined and nonvolatile manner at room temperature without the motion of any physical particles, this skyrmion logic system has the potential to deliver scalable high-speed low-power reversible Boolean and quantum computing.

DOI: 10.1103/PhysRevApplied.12.064053

I. INTRODUCTION

There is a fundamental minimum quantity of energy dissipated by a logic gate in which information-carrying signals are continuously created and destroyed, as determined by Landauer [1]. Reversible computing aims to circumvent this limitation by conserving information - and therefore energy - as signals propagate through a logic circuit [2]. In this scheme, conservative logical operations are executed through dissipation-free elastic interactions among these information carriers that conserve momentum and energy [3]. While Fredkin and Toffoli's original thought experiment considered billiard balls as the information carriers, Prakash *et al.* recently demonstrated conservative logic experimentally with micron-sized droplets driven through planar computing structures by pressure [4] and magnetism [5]. However, the large dimensions of the information carriers in these demonstrations detract

from the system efficiency and limit potential utility; a nanoscale information carrier for reversible computing remains elusive.

Magnetic skyrmions [6] are intriguing information carriers for reversible computing due to their small diameter (~ 50 nm at room temperature, below 20 nm at low temperature) [7–10] and the small current required to induce skyrmion motion [11]. These quasiparticles are topologically stable regions of magnetization that comprise a central core oriented antiparallel to the bulk of a magnetic structure [12–14]. Skyrmion motion involves the propagation of magnetization rather than the transport of physical particles, and can be induced by the spin Hall effect through the application of an electrical current [15]. These skyrmion quasiparticles move not along the axis of an electrical current, but rather deviate from this axis due to the skyrmion Hall effect, which is equivalent to the Magnus effect [16,17]. The skyrmion Hall effect is generally deleterious to device functionality, so a track structure, as shown in Fig. 1, is often used to suppress the skyrmion Hall effect and restrict motion to a single dimension

*joseph.friedman@utdallas.edu

†These authors contributed equally to this work.

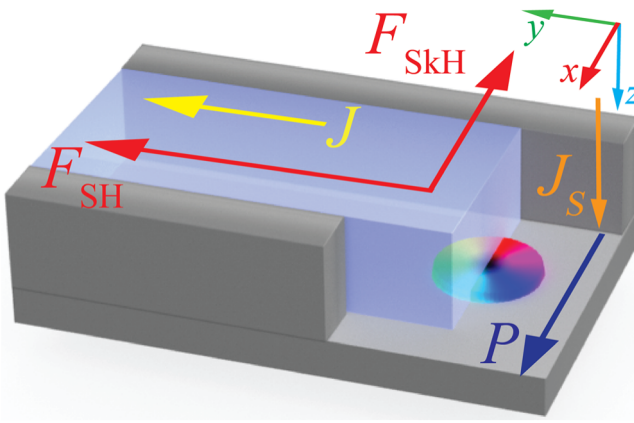


FIG. 1. Skyrmion track structure. Skyrmions propagate along a track comprised of Pt heavy metal (blue) and Co ferromagnet (gray, with polarization P), where an interfacial spin-orbit coupling induces a Dzyaloshinskii-Moriya interaction. This spin-orbit coupling also causes the externally-applied electrical current (J) flowing through the heavy metal in the $+y$ direction to create a spin current (J_S) polarized in the $+z$ direction via the spin Hall effect. The skyrmion (multicolor circle) lies in the ferromagnetic layer at the interface with the heavy metal, and the surrounding ferromagnet walls prevent the skyrmion from leaving the track. Spin current in the $+z$ direction produces a force F_{SH} on the skyrmions in the $+y$ direction, which is the direction of the electrical current. The track constriction prevents the $-x$ -directed skyrmion Hall force F_{SKH} from influencing the skyrmion trajectory. Note that the axes are inverted for visual clarity; the Pt heavy metal is below the Co ferromagnet.

[18–21]. Magnetic skyrmions propagating along ferromagnetic nanowire tracks [22,23] have been proposed for memory storage and individual logic gates [24–29], but the development of a scalable skyrmion computing system has been impeded by the need to directly cascade skyrmion logic gates without control and amplification circuitry that significantly reduces the system efficiency. Furthermore, previous skyrmion logic proposals require the continual creation and annihilation of skyrmions, which is an energetically expensive process that requires an external control system.

We therefore propose a reversible skyrmion logic system in which skyrmions are conserved as they flow through nanowire tracks. Logical operations are performed by thoroughly leveraging the rich physics of magnetic skyrmions: the spin Hall effect [15], the skyrmion Hall effect [16,17,30], skyrmion-skyrmion repulsion [31], repulsion between skyrmions and the track boundaries [31], and electrical current control of notch depinning [11]. Binary information is encoded by the presence (“1”) or absence (“0”) of magnetic skyrmions, with the skyrmions flowing directly from the output nanowire track of one logic gate to the input track of another logic gate without an external control or amplification circuit. These reversible skyrmion logic gates can provide FAN-OUT and be integrated into

a large-scale system, with signal integrity provided by simple electronic clock pulses applied to the entirety of the system. This logic-in-memory computing system is nonvolatile due to the topological stability and ferromagnetic nature of skyrmions, providing efficient pipelining that enhances the potential for high speed and low power. Furthermore, the availability of a Fredkin gate inspires the consideration of quantum computing with magnetic skyrmions.

II. MICROMAGNETIC SIMULATION METHODOLOGY

A. Micromagnetic simulation technique

The Landau-Lifshitz-Gilbert (LLG) equation of motion describes magnetization dynamics in ferromagnetic materials:

$$\frac{\partial \mathbf{M}}{\partial t} = -\gamma(\mathbf{M} \times \mathbf{H}_{\text{eff}}) + \frac{\alpha}{M_s} \left(\mathbf{M} \times \frac{\partial \mathbf{M}}{\partial t} \right) + \tau_{\text{CPP}}, \quad (1)$$

where \mathbf{M} is the magnetization vector, γ is the gyro-magnetic ratio, M_s is the saturation magnetization, and α is the Gilbert damping parameter. \mathbf{H}_{eff} is the effective field, which includes Heisenberg exchange, magneto-crystalline anisotropy, magnetostatic, Dzyaloshinskii-Moriya exchange, and external magnetic fields. τ_{CPP} implements the injection of spin Hall current perpendicularly to the sample and is described by

$$\tau_{\text{CPP}} = -\beta \epsilon' (\mathbf{M} \times \mathbf{m}_P) - \frac{\beta}{M_s} [\mathbf{M} \times (\mathbf{m}_P \times \mathbf{M})], \quad (2)$$

with \mathbf{m}_P as the spin Hall polarization direction and $\beta = (\theta_{\text{SH}} \hbar J / 2M_s e t_{\text{Co,track}})$, where θ_{SH} is the spin Hall angle, e is the electronic charge, J is the electrical current density, and $t_{\text{Co,track}}$ is the thickness of the Co track. ϵ' is the fieldlike torque, which is here considered to be zero; modifications to the skyrmion profile by that homogeneous in-plane field are not considered.

Simulations are therefore performed using MUMAX3, an open-source GPU-accelerated micromagnetic simulation software [32] that integrates the LLG equation of motion with a finite difference approach. We discretize the sample into cuboid cells, the dimensions of which are set to $1 \times 1 \times 0.4 \text{ nm}^3$, and we neglect thermal fluctuations by setting the temperature to 0 K. The zero-temperature simulation results are predictive of room-temperature experimental behavior of the proposed computing system, in which a randomly fluctuating thermal field will impact the skyrmion motion; as described in Sec. V A, notch synchronizers are used to prevent this random motion from causing logical errors. Furthermore, these phenomena have been suppressed experimentally in multilayer structures [33],

and the effect of this thermal field will be small relative to the applied electrical current.

B. Magnetic parameter selection

The following numerical values, which are adopted from Purnama *et al.* [18], model a multilayer of Pt and Co: saturation magnetization $M_s = 5.80 \times 10^5$ A/m, exchange stiffness $A_{\text{ex}} = 1.5 \times 10^{-11}$ J/m, Gilbert damping coefficient $\alpha = 0.1$, Dzyaloshinskii-Moriya interaction (DMI) constant $D_{\text{int}} = 3.0 \times 10^{-3}$ J/m², magnetocrystalline anisotropy constants $K_{u1} = 6 \times 10^5$ J/m³ and $K_{u2} = 1.5 \times 10^5$ J/m³, and spin polarization in the transverse direction $\mathbf{m}_P = (1, 0, 0)$. The anisotropy direction points upwards. The spin Hall angle θ_{SH} is considered to be equal to one. The thickness of the Pt layer is $t_{\text{Pt}} = 0.4$ nm and the thickness of the Co layer varies between $t_{\text{Co,track}} = 0.4$ nm (Fig. 1) and $t_{\text{Co,sample}} = 0.8$ nm elsewhere. As the skyrmions travel in lithographically-feasible 20-nm-wide nanowire tracks [34], they are confined to slightly smaller dimensions in a manner similar to the confinement shown in Ref. [9], where geometric confinement results in skyrmions with diameters of roughly 50 nm.

III. REVERSIBLE SKYRMION LOGIC GATES

A. Reversible skyrmion AND/OR gate

The reversible AND/OR logic function described in Table I is the primary workhorse of the proposed skyrmion computing system. As this function is reversible, the total number of skyrmions, N , provided to inputs A and B is always equal to the total number of skyrmions emitted by the AND and OR outputs. This reversible logic function is performed by the structure shown in Fig. 2, with micromagnetic simulations [32] depicting the skyrmion trajectories for each input combination (see the Supplemental Material [35]). The spin Hall effect pushes the skyrmions in the $+y$ direction through the vertical tracks of Fig. 1, while the skyrmion Hall effect introduces a $-x$ -directed force that is mediated by repulsion from the track boundaries. The skyrmions are therefore free to move laterally within the central junction, where the skyrmion Hall effect causes leftward skyrmion propagation unless repulsed by a second skyrmion.

Whenever a skyrmion enters one of the input ports of the AND/OR gate, this logic gate geometry forces a skyrmion

TABLE I. Truth table for the AND/OR gate.

Inputs		N	Outputs	
A	B		AND	OR
0	0	0	0	0
0	1	1	0	1
1	0	1	0	1
1	1	2	1	1

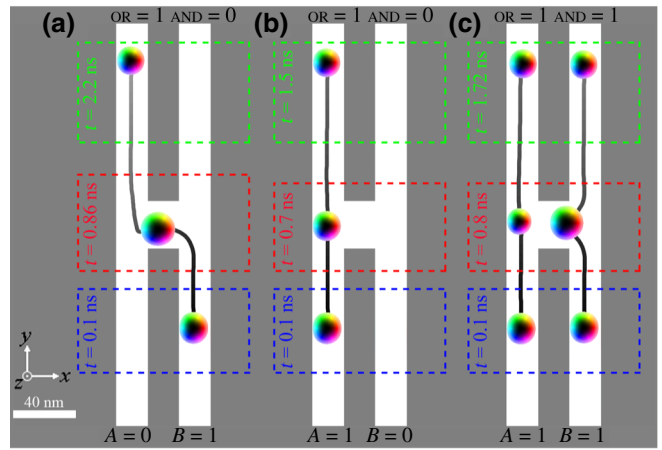
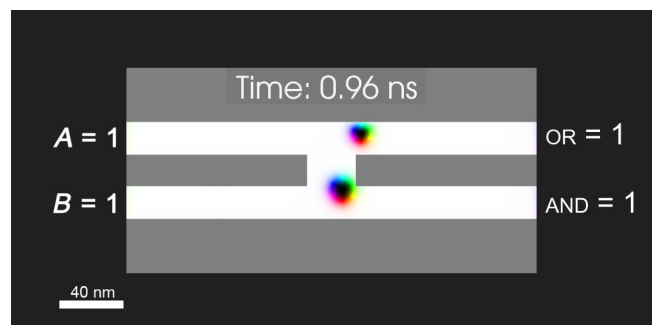


FIG. 2. Micromagnetic simulation results for the AND/OR gate are shown for input combinations (a) $A = 0, B = 1$; (b) $A = 1, B = 0$; and (c) $A = B = 1$. In this and other figures, the path of each skyrmion is shown as a grayscale line that is black at $t = 0$ and gradually lightens as the simulation advances, with skyrmion snapshots provided at the times noted in the figure. The spin current J_S resulting from constant electrical current $J = 5 \times 10^{10}$ A/m² pushes the skyrmions in the $+y$ direction, with a skyrmion Hall force directed in the $-x$ direction. Therefore, when confined laterally by their tracks, the input skyrmions travel directly in the $+y$ direction until they reach the central junction. In the lateral opening of the constrictive tracks at the central junction, the skyrmion Hall force induces a $-x$ -directed component to the skyrmion trajectory that is counteracted by skyrmion-skyrmion repulsion.

to propagate to the OR output port to represent binary “1.” If two skyrmions are input to this logic gate, one skyrmion is emitted by the OR output port and the other skyrmion is emitted by the AND output port, such that both produce binary “1.” Finally, if no skyrmions enter either input port, then no skyrmions are emitted by either output port, representing binary “0” outputs. The operation of the AND/OR gate is shown in Video 1 for these



VIDEO 1. Micromagnetic simulation of AND/OR logic gate with input combinations (a) $A = 0, B = 1$; (b) $A = 1, B = 0$; and (c) $A = B = 1$. This video is analogous to Fig. 2.

TABLE II. Truth table for the INV/COPY gate.

Inputs			Outputs		
CTRL	IN	N	COPY1	NOT	COPY2
1	0	1	0	1	0
1	1	2	1	0	1

three input combinations. The combined forces resulting from the spin Hall effect, the skyrmion Hall effect, skyrmion-skyrmion repulsion, and repulsion between the skyrmions and the boundaries thus cause this structure to simultaneously calculate the logical functions $A \vee B$ and $A \wedge B$ while conserving the skyrmions.

B. Reversible skyrmion INV/COPY gate

The inclusion of an inversion operation enables the generation of all possible Boolean logic functions, which cannot be achieved by the AND and OR operations alone. The proposed INV/COPY gate shown in Table II, Fig. 3, and Video 2 functions similarly to the AND/OR gate shown above, here with an additional output port and the requirement that a skyrmion always be provided to the control (CTRL) input. (see Fig. S1, Table S1, and Video S1 within the Supplemental Material for the behavior when CTRL is “0” [35].) This reversible INV/COPY gate simultaneously duplicates and inverts the skyrmion input signal. As shown in Table II, the NOT output is therefore “1” whenever the IN input is “0,” and “0” whenever the IN input is “1.” This reversible logic gate also performs the FAN-OUT function, through which skyrmions are conserved such that the IN signal is duplicated to the two COPY outputs. This signal duplication is an essential component of a large-scale

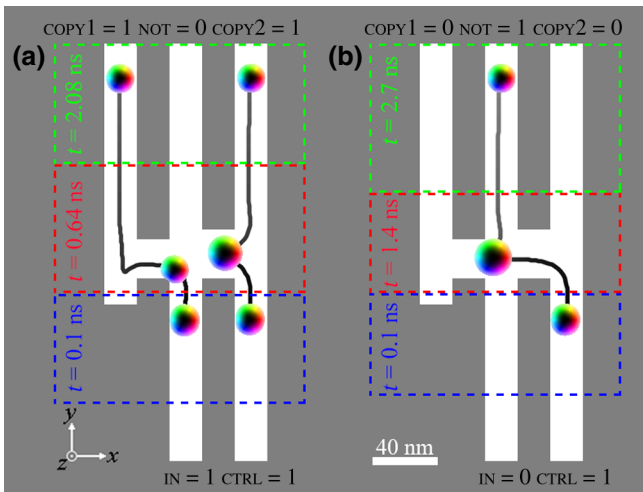


FIG. 3. Micromagnetic simulation results for the INV/COPY gate are shown for input combinations (a) IN = 1, CTRL = 1; and (b) IN = 0; CTRL = 1.



VIDEO 2. Micromagnetic simulation of INV/COPY logic gate for IN = 1 and IN = 0. In order to provide the inversion and duplication behaviors, CTRL = 1 in both simulations. This video is analogous to Fig. 3.

computing system, and can be performed repeatedly by cascaded INV/COPY gates to generate numerous copies of a signal.

IV. POTENTIAL FOR SKYRMION QUANTUM COMPUTATION

A magnetic skyrmion quantum computing system can be envisioned in which quantum non-binary operators operate in concert with the binary operations of a skyrmion Fredkin gate. In particular, the availability of atomic-scale skyrmions [7,36] and the fact that skyrmions coupled to conventional superconductors support Majorana fermions [37] open a pathway to topological quantum computation [38,39]. Building on our proposed skyrmion Fredkin gate and various potential physical solutions for qubit encoding and manipulation, we propose two quantum gate sets for a universal skyrmion quantum computing system: one based on the conventional combination of Toffoli and Hadamard gates, and the other based on Clifford and T gates.

A. Skyrmion Fredkin gate

In addition to reversible Boolean computation, this skyrmion logic system has potential applications in quantum computation. As single-spin states are promising candidates for qubits, the recent experimental demonstration of atomic-scale magnetic skyrmions provides a potential pathway to quantum computing with skyrmion qubits [7, 36]. We therefore propose in Fig. 4, Video 3, and Table III the reversible Fredkin gate implemented in this skyrmion logic paradigm. Here, skyrmions provided to the C input propagate to the O output and determine whether or not the I_1 and I_2 input signals are swapped as they travel to the O_1 and O_2 outputs (see also Fig. S2 within the Supplemental Material [35]). A controlled-NOT (CNOT) gate can also

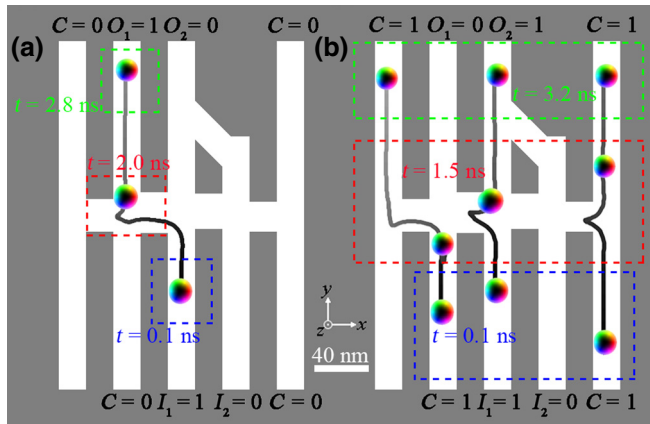
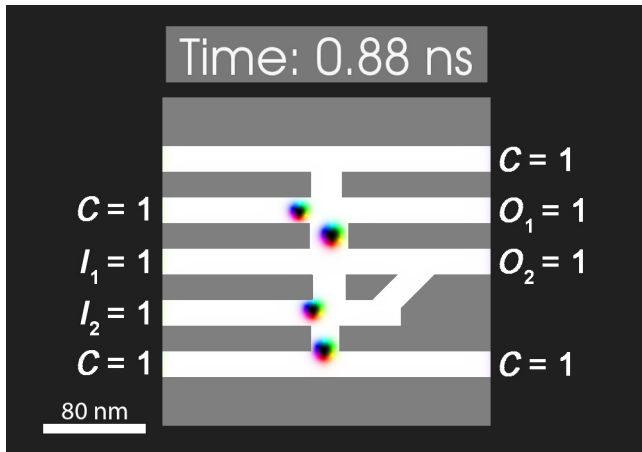


FIG. 4. Micromagnetic simulation results for the Fredkin gate. (a) When $C=0$, the input signals travel directly to the output ports without swapping; that is, $O_1=I_1$ and $O_2=I_2$. (b) When $C=1$, the input skyrmions swap paths such that $O_1=I_2$ and $O_2=I_1$. The C signal is duplicated, with both skyrmions at the C input propagating directly to the C output.

be achieved, and is implicitly included in the full adder described in Sec. V B [Fig. 6].

B. Toffoli + Hadamard universal quantum gate set

The Fredkin gate is an intermediary between classical Boolean logic and full/universal quantum logic, and three Fredkin gates can be cascaded to realize a Toffoli gate. As a Toffoli gate in concert with a Hadamard gate are quantum computationally universal, the only missing component required for quantum computing within this skyrmion logic system is the Hadamard gate. The availability of multiple types of skyrmions (antiferromagnetic, etc.) opens a pathway to achieve a skyrmion Hadamard



VIDEO 3. Micromagnetic simulation of Fredkin gate for all nontrivial input combinations. This video is analogous to Fig. 4 and Fig. S2.

TABLE III. Truth table for the Fredkin gate.

Inputs			Outputs			
C	I_1	I_2	N	C	O_1	O_2
0	0	0	0	0	0	0
0	0	1	1	0	0	1
0	1	0	1	0	1	0
0	1	1	2	0	1	1
1	0	0	2	1	0	0
1	0	1	3	1	1	0
1	1	0	3	1	0	1
1	1	1	4	1	1	1

gate analogous to an optical beam splitter with half probability. Here, when a “gate skyrmion” interacts with a “qubit skyrmion,” the “gate skyrmion” changes the state of the “qubit skyrmion.” The “gate skyrmion” represents the unitary transformation of the quantum Hadamard gate, creating an equal superposition between two possible positions of a particle (the “qubit skyrmion”). “Qubit skyrmions” may be left initialized in “0” or “1” states, which are represented by the absence or presence of a skyrmion, respectively, as described throughout the text. This Hadamard gate thus provides the necessary quantum state superposition.

C. Clifford + T universal quantum gate set

Given their high number of spins and intrinsic topological properties, skyrmions are intrinsically quantum-error-corrected logical qubits. It may therefore be feasible to consider the quantum universal Clifford + T gate-set [40], in which all skyrmions are qubit carriers. The single qubit T gate can act on individual skyrmions (qubits), while the Clifford gates (efficient to simulate on a classical computer) are implemented by interacting the skyrmions [37]. The most observed and investigated skyrmions are two-dimensional, which suggests that these Clifford gates may be implemented by braiding the movement trajectories of the skyrmions in a manner similar to that of conventional surface quantum-error-correcting code [41].

V. LARGE-SCALE INTEGRATED SKYRMION COMPUTING SYSTEM

While these reversible logic gates are interesting in their own right, a mechanism for cascading logic gates is necessary for practical computing applications. In the proposed reversible computing system, the output skyrmions emitted by one logic gate are used as input skyrmions for another gate. As the logic gate functionality is based on skyrmion interactions at the central junctions, a synchronization mechanism must also be provided to ensure that skyrmions arriving from different input paths reach the central junction simultaneously, despite thermal effects.

A. Notch synchronization with global clock

This synchronization is achieved with the notch structure [11] of Fig. 5(b) by applying a large spin Hall current pulse that enables the skyrmions to traverse the notch only when this large pulse is applied. This large current pulse causes a decrease in skyrmion diameter, while also increasing the skyrmion velocity, as shown in Fig. 5(a). As depicted in Fig. 5(c) and Video 4, a small spin Hall current is continuously applied to the entire system to propagate the skyrmions through the tracks and logic gate junctions; this current magnitude is below the threshold required for skyrmions to traverse the notches. At regular intervals, a large spin Hall current pulse is provided to the entire system to drive the skyrmions past the notches; this regular pulse represents the global system clock that synchronizes the computing system. These notch synchronizers can be placed following the output of a logic gate, with the IN port of the notch synchronizer connected to an output port of a logic gate; the OUT port of the notch synchronizer is connected to an input port of a cascaded logic gate. Notches are inserted between every logic gate input and output where synchronization is required, with each notch synchronizer handling zero or one skyrmion during each clock cycle. Alternatively, this synchronization can be similarly

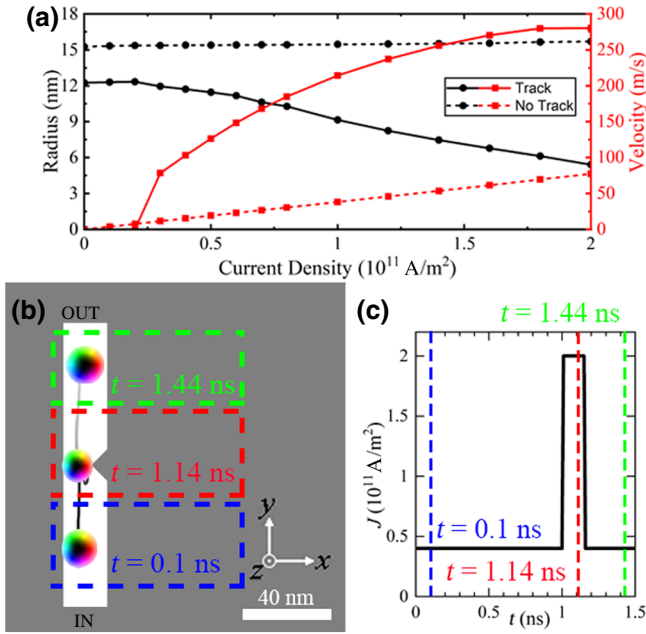
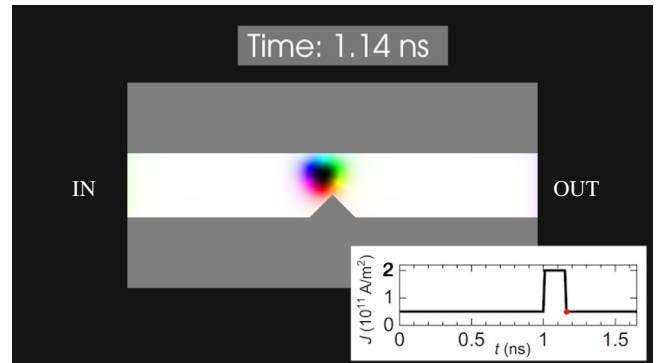


FIG. 5. Signal synchronization. (a) Skyrmiion radius as a function of applied electrical current density. (b) A 7-nm-wide notch is formed in the 20-nm-wide nanowire track to create a constriction that permits skyrmion passage only when a large current is applied. (c) The electrical current applied to the entirety of the computing system maintains a constant low magnitude of $J = 5 \times 10^{10} \text{ A/m}^2$, which is periodically amplified to $J = 2 \times 10^{11} \text{ A/m}^2$ for 150 ps to enable skyrmions to traverse notches throughout the system. The skyrmion traverses the notch when this large clock pulse is applied at $t = 1 \text{ ns}$.



VIDEO 4. Micromagnetic simulation of notch structure that synchronizes the skyrmions flowing through various portions of the circuit. This video is analogous to Fig. 5.

achieved through clocked electrical control of the magnetic anisotropy [42].

B. Directly-cascaded skyrmion logic gates

Integrating the basis logic gates with the cascading and synchronization mechanisms enables the scaling of this reversible computing paradigm to large systems that efficiently perform complex functions. An example is provided in Fig. 6 and Video 5, where the input A , B , and carry-in skyrmion signals interact as they propagate

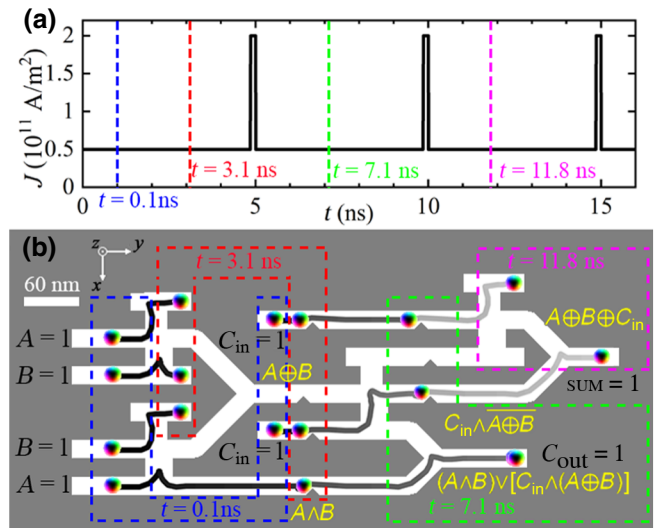
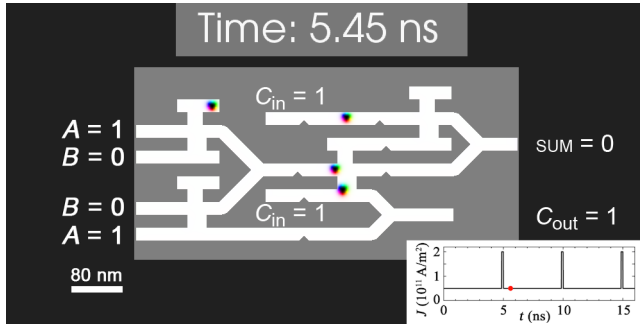


FIG. 6. Cascaded one-bit full adder. (a) Cascaded logic gates are synchronized by large 150-ps-wide electrical pulses applied to the entire structure with a clock period of 5 ns. (b) A one-bit full adder computes the binary SUM and carry-out of two one-bit binary numbers, A and B , and a carry-in bit. The notches ensure that the skyrmions are synchronized with one another as they enter each logic gate, thereby providing proper skyrmion-skyrmion repulsion and logical functionality. After two (three) clock cycles, the skyrmion signals reach the C_{out} (SUM) output.



VIDEO 5. Micromagnetic simulation of one-bit full adder for all nontrivial input combinations. This video is analogous to Fig. 6 and Fig. S4.

through the circuit to produce the sum and carry-out skyrmion signals, thus executing the one-bit full-addition function with two half adders (half adder simulations are found in Fig. S3 and Video S2, the full adder truth table is given in Table S2, and simulation results for all full adder input combinations are found in Fig. S4 within the Supplemental Material [35]). A 150-ps-wide clock pulse is provided every 5 ns to synchronize the skyrmions, ensuring proper conservative logic interactions within each component logic gate. The SUM output is produced within three clock cycles, while the carry-out output is produced within two clock cycles; the carry-in to carry-out delay is only one clock cycle. These clocked skyrmion signals provide a natural means for pipelining, enabling the execution of n -bit addition within $n + 2$ clock cycles; this pipelining procedure can be observed in Fig. 7 and Video 6. Furthermore, although the 200 MHz clock frequency and the electrical current magnitudes used in simulation provide inferior efficiency to that of conventional computing systems, the nonvolatility and pipelining inspire a vision for highly-efficient computing with alternative materials [43] and improvements in the Rashba coefficient and spin Hall angle [44].

VI. EXPERIMENTAL APPROACHES

The skyrmion logic system proposed here is experimentally feasible with industrially relevant magnetic multilayers of the required material systems at lithographically-accessible length scales. Furthermore, room-temperature field-free operation is achievable, as nanoscale chiral skyrmions were recently stabilized at room temperature with zero magnetic field [33,45,46]. Similar to the material parameters used in the above micromagnetic simulations, a Co-based multilayer (Ir/Pt/Co) stack, grown by sputtering, has been proposed that should enable room-temperature sub-100-nm skyrmions stabilized by a large additive DMI [33]. By further tuning material parameters, such as the perpendicular anisotropy, the thickness of the magnetic layers, or the DMI, even smaller skyrmion

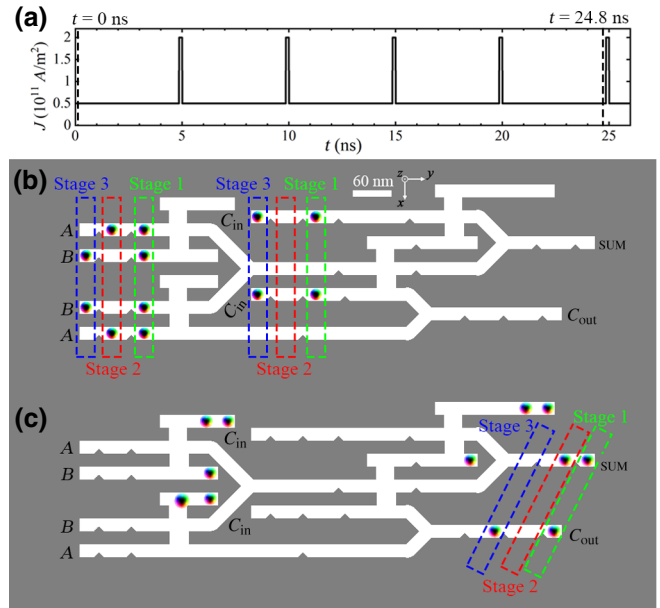
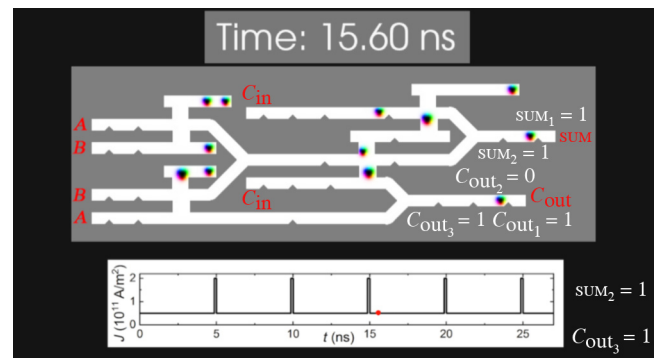


FIG. 7. Pipelined full adder. The clocked full adder structure can be used for pipelined operations such that each logic gate junction is used within each clock cycle. (a) The clocking scheme used in the full adder micromagnetic simulation is extended for five cycles to perform three separate full adder operations simultaneously. (b) The initial state ($t = 0$ ns) of a three-stage pipeline is shown here for the following inputs: in stage one, $A = B = C_{\text{in}} = 1$; in stage two, $A = 1$ and $B = C_{\text{in}} = 0$; and in stage three, $A = 0$ and $B = C_{\text{in}} = 1$. (c) The final state ($t = 24.8$ ns) is seen after five clock cycles, with the following results: for stage one, $\text{SUM} = C_{\text{out}} = 1$; for stage two, $\text{SUM} = 1$ and $C_{\text{out}} = 0$; and for stage three, $\text{SUM} = 0$ and $C_{\text{out}} = 1$. The entirety of the simulation is shown in Video 6.

dimensions can be achieved [11]. Full-field x-ray magnetic imaging techniques can be used to demonstrate the device functionality and logic operations, including full-field magnetic transmission soft-x-ray microscopy (MTXM) or photoemission electron microscopy (PEEM), which is a



VIDEO 6. Micromagnetic simulation of pipelined full adder demonstrating the ability to provide a throughput of one full addition per clock cycle despite the two- and three-cycle latencies to produce the carry-out and SUM outputs, respectively. This video is analogous to Fig. 7.

full-field surface-sensitive x-ray imaging technique. X-ray imaging is magnetization-sensitive and nondisruptive to the sample. For the proposed system in particular, imaging of the magnetic states of the devices must utilize the x-ray magnetic circular dichroism (XMCD) effect and tune the incoming photon energy to the Co L_3 edge (~ 779 eV).

A. Skyrmion generation

In a fully reversible skyrmion logic system, skyrmions must only be generated once: at the beginning of the system operation. After these initial skyrmions are generated, they are continually propagated through the logic gates such that the output skyrmions of each conservative skyrmion logic gate are used as the input skyrmions of other conservative skyrmion logic gates (see Sec. VI C). These skyrmions generated at system initialization are therefore sufficient for long-term use of this system, and their nonvolatility enables the skyrmions to maintain their states even when the power supply is removed.

As skyrmion generation is significantly more challenging than the generation of many other types of information carriers, this ability to conserve skyrmions marks a major advance in comparison to previous proposals for skyrmion logic [24–29]. As this reversible computing system requires only a single skyrmion initialization process, the precise technique used has limited impact on the overall system efficiency. Several techniques are available, with the application of nanosecond electrical current pulses [8] appearing particularly promising.

Alternatively, ease-of-demonstration as well as optimization of the conventional metrics of speed, power, and delay may inspire a compromise regarding the conservation of skyrmions. Another approach to skyrmion generation is to continually generate skyrmions at specific points within the system with a dedicated skyrmion generation structure. This can be achieved with homogeneous currents [8] or with nanosecond electrical current pulses, as achieved in Ref. [47] for a device-compatible stripline geometry. This skyrmion generator will generate a skyrmion in each clock cycle, which then can be provided as an input to a particular logic gate where an input skyrmion is always required (e.g., for the CTRL input of the INV/COPY gate). These skyrmions will then travel through the circuit and eventually be annihilated after they have performed the desired operations. While this alternative system will no longer be fully reversible, the simplicity of this approach may be advantageous for proof-of-concept experiments and eventual high-performance computing systems.

B. Skyrmion detection

To read the binary outputs of this conservative logic system, it is necessary to detect the presence (binary “1”) or absence (binary “0”) of skyrmions at various

points throughout the circuit. While standard magnetic force microscopy imaging can be used to detect skyrmions in a laboratory setting, computing applications require transformation of the skyrmion information into electrical signals. Determination of the presence or absence of a skyrmion at a particular location can be achieved by placing a tunneling barrier and hard ferromagnet above the Co ferromagnet to form a magnetic tunnel junction (MTJ), as described in previous logic and memory proposals with domain walls and skyrmions [25,27,29]. The magnetoresistance of this MTJ indicates the presence or absence of a skyrmion within the free layer, as the skyrmion modifies the local magnetization within the free layer and therefore the current through the MTJ tunneling barrier.

C. Skyrmion conservation

While each of the skyrmion logic gates conserves skyrmions by propagating each input skyrmion to an output port, the operation of a complete conservative logic system requires the conservation of skyrmions throughout the system. It is therefore critical that every skyrmion transmitted to the output port of a skyrmion logic gate is then used as an input to another skyrmion logic gate.

As can be observed in relation to the full adder of Fig. 6, skyrmions propagate to several superfluous output ports that contain logical byproducts of the computation of the SUM and carry-out signals. In particular, the full adder also produces the signals A , B , $A \wedge B$, C_{in} , and $C_{\text{in}} \wedge (A \oplus B)$; these signals are byproducts of the full adder computation that are not the primary objectives of the full adder circuit. These signals are therefore available for use in other logic gates; it may be noted that one signal is available at the output for each of the three input signals.

To enable a reversible system, these skyrmion signals must be able to propagate to other logic gates. As the lateral flow of information through this two-dimensional structure is unidirectional (left to right), it is necessary to provide a technique by which skyrmions are provided to the left side of the circuit. Many potential techniques may be available, such as the use of an additional circuit layer, which would also enable the interaction-free crossover of skyrmion tracks. Furthermore, the direction of the spin current can be modified through static or dynamic modulation of the electrical current direction or the ferromagnetic Co magnetization. Finally, it should be noted that it may be worthwhile to shed the requirement of complete skyrmion conservation in order to maximize the primary metrics of a computing system (energy consumption, processing speed, and area footprint).

VII. CONCLUSIONS

The proposed skyrmion structure enables the realization of a nanoscale reversible computing system with nearly

ideal characteristics. Small spin Hall currents are supplied and the energy required for motion approaches the reversible computing ideal of frictionless information propagation. Rather than avoiding the skyrmion Hall effect, the proposed system leverages the rich physics of magnetic skyrmions to provide cascaded logic operations that are pipelined and synchronized to maintain signal integrity when scaled to large systems. In addition to Boolean logic, the availability of a Fredkin gate inspires a vision for quantum computing with magnetic skyrmions. Furthermore, the stability of the ferromagnetic materials provides nonvolatility that can be exploited in non-von Neumann architectures that overcome the limitations of conventional computing systems. By performing conservative logic with magnetic skyrmions, the proposed system enables a reversible computing paradigm that approaches the ultimate thermodynamic limits of information processing efficiency.

ACKNOWLEDGMENTS

The authors thank H.-J. Drouhin for arranging the research exchange and M. R. Stan for fruitful discussions.

-
- [1] R. Landauer, Irreversibility and heat generation in the computing process, *IBM J. Res. Dev.* **5**, 183 (1961).
- [2] T. Toffoli, in *ICALP* (1980), pp. 632–644.
- [3] E. Fredkin and T. Toffoli, Conservative logic, *Int. J. Theor. Phys.* **21**, 219 (1982).
- [4] M. Prakash and N. Gershenfeld, Microfluidic bubble logic, *Science* **315**, 832 (2007).
- [5] G. Katsikis, J. S. Cybulski, and M. Prakash, Synchronous universal droplet logic and control, *Nat. Phys.* **11**, 588 (2015).
- [6] T. H. R. Skyrme, A unified field theory of mesons and baryons, *Nucl. Phys.* **31**, 556 (1962).
- [7] S. Heinze, K. Von Bergmann, M. Menzel, J. Brede, A. Kubetzka, R. Wiesendanger, G. Bihlmayer, and S. Blügel, Spontaneous atomic-scale magnetic skyrmion lattice in two dimensions, *Nat. Phys.* **7**, 713 (2011).
- [8] W. Legrand, D. Maccariello, N. Reyren, K. Garcia, C. Moutafis, C. Moreau-Luchaire, S. Collin, K. Bouzehouane, V. Cros, and A. Fert, Room-temperature current-induced generation and motion of sub-100 nm skyrmions, *Nano Lett.* **17**, 2703 (2017).
- [9] P. Ho, A. K. C. Tan, S. Goolaup, A. L. G. Oyarce, M. Raju, L. S. Huang, A. Soumyanarayanan, and C. Panagopoulos, Geometrically Tailored Skyrmions at Zero Magnetic Field in Multilayered Nanostructures, *Phys. Rev. Appl.* **11**, 024064 (2019).
- [10] S. Meyer, M. Perini, S. von Malottki, A. Kubetzka, R. Wiesendanger, K. von Bergmann, and S. Heinze, Isolated zero field sub-10 nm skyrmions in ultrathin Co films, *Nat. Commun.* **10**, 3823 (2019).
- [11] J. Sampaio, V. Cros, S. Rohart, A. Thiaville, and A. Fert, Nucleation, stability and current-induced motion of isolated magnetic skyrmions in nanostructures, *Nat. Nanotechnol.* **8**, 839 (2013).
- [12] S. Mühlbauer, B. Binz, F. Jonietz, C. Pfleiderer, A. Rosch, A. Neubauer, R. Georgii, and P. Boni, Skyrmion lattice in a chiral magnet, *Science* **323**, 915 (2009).
- [13] W. Münzer, A. Neubauer, T. Adams, S. Mühlbauer, C. Franz, F. Jonietz, R. Georgii, P. Böni, B. Pedersen, M. Schmidt, A. Rosch, and C. Pfleiderer, Skyrmion lattice in the doped semiconductor $\text{Fe}_{1-x}\text{Co}_x\text{Si}$, *Phys. Rev. B* **81**, 041203 (2010).
- [14] A. Fert, N. Reyren, and V. Cros, Magnetic skyrmions: Advances in physics and potential applications, *Nat. Rev. Mater.* **2**, 17031 (2017).
- [15] J. Sinova, S. O. Valenzuela, J. Wunderlich, C. H. Back, and T. Jungwirth, Spin Hall effects, *Rev. Mod. Phys.* **87**, 1213 (2015).
- [16] W. Jiang, X. Zhang, G. Yu, W. Zhang, X. Wang, M. Benjamin Jungfleisch, J. E. Pearson, X. Cheng, O. Heinonen, K. L. Wang, Y. Zhou, A. Hoffmann, and S. G. E. te Velthuis, Direct observation of the skyrmion Hall effect, *Nat. Phys.* **13**, 162 (2017).
- [17] K. Litzius, I. Lemesh, B. Krüger, P. Bassirian, L. Caretta, K. Richter, F. Büttner, K. Sato, O. A. Tretiakov, J. Förster, R. M. Reeve, M. Weigand, I. Bykova, H. Stoll, G. Schütz, G. S. D. Beach, and M. Kläui, Skyrmion Hall effect revealed by direct time-resolved X-ray microscopy, *Nat. Phys.* **13**, 170 (2017).
- [18] I. Purnama, W. L. Gan, D. W. Wong, and W. S. Lew, Guided current-induced skyrmion motion in 1D potential well, *Sci. Rep.* **5**, 10620 (2015).
- [19] X. Zhang, Y. Zhou, and M. Ezawa, Magnetic bilayer-skyrmions without skyrmion Hall effect, *Nat. Commun.* **7**, 10293 (2016).
- [20] J. Barker and O. A. Tretiakov, Static and Dynamical Properties of Antiferromagnetic Skyrmions in the Presence of Applied Current and Temperature, *Phys. Rev. Lett.* **116**, 147203 (2016).
- [21] X. Zhang, Y. Zhou, and M. Ezawa, Antiferromagnetic skyrmion: Stability, creation and manipulation, *Sci. Rep.* **6**, 24795 (2016).
- [22] R. Tomasello, E. Martinez, R. Zivieri, L. Torres, M. Carpentieri, and G. Finocchio, A strategy for the design of skyrmion racetrack memories, *Sci. Rep.* **4**, 6784 (2014).
- [23] A. Fert, V. Cros, and J. Sampaio, Skyrmions on the track, *Nat. Nanotechnol.* **8**, 152 (2013).
- [24] S. Zhang, A. A. Baker, S. Komineas, and T. Hesjedal, Topological computation based on direct magnetic logic communication, *Sci. Rep.* **5**, 15773 (2015).
- [25] X. Zhang, M. Ezawa, and Y. Zhou, Magnetic skyrmion logic gates: Conversion, duplication and merging of skyrmions, *Sci. Rep.* **5**, 9400 (2015).
- [26] X. Zhang, Y. Zhou, M. Ezawa, G. P. Zhao, and W. Zhao, Magnetic skyrmion transistor: Skyrmion motion in a voltage-gated nanotrack, *Sci. Rep.* **5**, 11369 (2015).
- [27] Z. He, S. Angizi, and D. Fan, Current-induced dynamics of multiple skyrmions with domain-wall pair and skyrmion-based majority gate design, *IEEE Magn. Lett.* **8**, 4305705 (2017).
- [28] X. Xing, P. W. T. Pong, and Y. Zhou, Skyrmion domain wall collision and domain wall-gated skyrmion logic, *Phys. Rev. B* **94**, 054408 (2016).

- [29] S. Luo, M. Song, X. Li, Y. Zhang, J. Hong, X. Yang, X. Zou, N. Xu, and L. You, Reconfigurable skyrmion logic gates, *Nano Lett.* **18**, 1180 (2018).
- [30] S. Z. Lin, C. Reichhardt, C. D. Batista, and A. Saxena, Particle model for skyrmions in metallic chiral magnets: Dynamics, pinning, and creep, *Phys. Rev. B* **87**, 214419 (2013).
- [31] X. Zhang, G. P. Zhao, H. Fangohr, J. P. Liu, W. X. Xia, J. Xia, and F. J. Morvan, Skyrmion-skyrmion and skyrmion-edge repulsions in skyrmion-based racetrack memory, *Sci. Rep.* **5**, 7643 (2015).
- [32] A. Vansteenkiste, J. Leliaert, M. Dvornik, F. Garcia-Sanchez, and B. Van Waeyenberge, The design and verification of Mumax3, *AIP Adv.* **4**, 107133 (2014).
- [33] C. Moreau-Luchaire, C. Moutafis, N. Reyren, J. Sampaio, C. A. F. Vaz, N. Van Horne, K. Bouzehouane, K. Garcia, C. Deranlot, P. Warnicke, P. Wohlhüter, J.-M. George, M. Weigand, J. Raabe, V. Cros, and A. Fert, Additive interfacial chiral interaction in multilayers for stabilization of small individual skyrmions at room temperature, *Nat. Nanotechnol.* **11**, 444 (2016).
- [34] D. Ravelosona *et al.*, in *Magn. Nano- Microwires Des. Synth. Prop. Appl.*, edited by M. Vazquez (Elsevier, New York, NY, USA, 2015), pp. 333–378.
- [35] See the Supplemental Material at <http://link.aps.org/supplemental/10.1103/PhysRevApplied.12.064053> for further details regarding the logical operations.
- [36] N. Romming, C. Hanneken, M. Menzel, J. E. Bickel, B. Wolter, K. von Bergmann, A. Kubetzka, and R. Wiesendanger, Writing and deleting single magnetic skyrmions, *Science* **341**, 636 (2013).
- [37] G. Yang, P. Stano, J. Klinovaja, and D. Loss, Majorana bound states in magnetic skyrmions, *Phys. Rev. B* **93**, 224505 (2016).
- [38] A. Roy and D. P. DiVincenzo, Topological quantum computing, [arXiv:1701.05052](https://arxiv.org/abs/1701.05052) (2017).
- [39] C. Psaroudaki, S. Hoffman, J. Klinovaja, and D. Loss, Quantum Dynamics of Skyrmions in Chiral Magnets, *Phys. Rev. X* **7**, 041045 (2017).
- [40] A. Paler, I. Polian, K. Nemoto, and S. J. Devitt, Fault-tolerant, high-level quantum circuits: Form, compilation and description, *Quantum Sci. Technol.* **2**, 25003 (2017).
- [41] R. Raussendorf and J. Harrington, Fault-Tolerant Quantum Computation with High Threshold in Two Dimensions, *Phys. Rev. Lett.* **98**, 190504 (2007).
- [42] W. Kang, Y. Huang, C. Zheng, W. Lv, N. Lei, Y. Zhang, X. Zhang, Y. Zhou, and W. Zhao, Voltage controlled magnetic skyrmion motion for racetrack memory, *Sci. Rep.* **6**, 23164 (2016).
- [43] A. R. Mellnik, J. S. Lee, A. Richardella, J. L. Grab, P. J. Mintun, M. H. Fischer, A. Vaezi, A. Manchon, E. A. Kim, N. Samarth, and D. C. Ralph, Spin-transfer torque generated by a topological insulator, *Nature* **511**, 449 (2014).
- [44] S. Emori, U. Bauer, S.-M. Ahn, E. Martinez, and G. S. D. Beach, Current-driven dynamics of chiral ferromagnetic domain walls, *Nat. Mater.* **12**, 611 (2013).
- [45] O. Boulle, J. Vogel, H. Yang, S. Pizzini, D. de S. Chaves, A. Locatelli, T. O. M. A. Sala, L. D. Buda-Prejbeanu, O. Klein, M. Belmeguenai, Y. Roussigné, A. Stashkevich, S. M. Chérif, L. Aballe, M. Foerster, M. Chshiev, S. Auffret, I. M. Miron, and G. Gaudin, Room temperature chiral magnetic skyrmion in ultrathin magnetic nanostructures, *Nat. Nanotechnol.* **11**, 449 (2016).
- [46] S. Woo, K. Litzius, B. Krüger, M.-Y. Im, L. Caretta, K. Richter, M. Mann, A. Krone, R. M. Reeve, M. Weigand, P. Agrawal, I. Lemesh, M.-A. Mawass, P. Fischer, M. Kläui, and G. S. D. Beach, Observation of room-temperature magnetic skyrmions and their current-driven dynamics in ultrathin metallic ferromagnets, *Nat. Mater.* **15**, 501 (2016).
- [47] S. Woo, K. M. Song, X. Zhang, M. Ezawa, Y. Zhou, X. Liu, M. Weigand, S. Finizio, J. Raabe, M.-C. Park, K.-Y. Lee, J. W. Choi, Y.-C. Min, H. C. Koo, and J. Chang, Deterministic creation and deletion of a single magnetic skyrmion observed by direct time-resolved X-ray microscopy, *Nat. Electron.* **1**, 288 (2018).